

# Effects of PZ Strength on Cyclic Seismic Performance of RBS Steel Moment Connections

## RBS 철골모멘트접합부의 내진성능에 대한 패널존 강도의 영향

이철호<sup>1)</sup> · 김재훈<sup>2)</sup>

Lee, Cheol-Ho · Kim, Jae-Hoon

**국문 요약** >> 보 플랜지 절취형(Reduced Beam Section, RBS) 내진 철골모멘트접합부는 국내외의 여러 실험프로그램에서 뛰어난 내진성능을 보여 주었다. 그러나 추가적으로 규명해야할 설계상의 몇몇 이슈들이 아직 남아있다. 그 중의 하나가 패널존의 보에 대한 적정강도이다. 다수의 실험결과가 존재함에도 불구하고 패널존과 보 사이의 적정강도비가 아직까지 명확하게 제시된 바가 없다. 본 연구에서는 독립적으로 수행된 국내외의 광범위한 실험 데이터베이스를 기초로 패널존 강도가 접합부의 내진거동에 미치는 영향을 포괄적으로 분석하였다. 이를 기초로 보의 좌굴을 감소시키는 동시에 충분한 접합부 소성회전능력을 보장할 수 있는 균형패널존의 강도범위를 제안하였다. 아울러 반복재하 실험대 실험결과를 만족스럽게 재현할 수 있는 유한요소모델을 구축한 후 다양한 수치해석을 통하여 실험자료에서 누락된 부분이나 실험적으로는 파악하기 어려운 거동을 고찰하였다. 이 과정에서 오늘날의 강력한 유한요소해석기법을 활용하여 많은 비용이 드는 철골접합부 실험대 내진실험을 보완하거나 적어도 부분적으로 대체할 수 있음을 확인하였다.

**주요어** 철골모멘트접합부, 패널존, 보 플랜지 절취형, 내진설계

**ABSTRACT** >> The reduced beam section (RBS) steel moment connection has performed well in past numerous tests. However there still remain several design issues that should be further examined. One such issue on RBS connection performance is the panel zone strength. Although a significant amount of test data are available, a specific recommendation for a desirable range of panel zone strength versus beam strength has yet to be proposed. In this paper, the effects of panel zone strength on the cyclic performance of RBS connection are investigated based on the available test database from comprehensive independent testing programs. A criterion for a balanced panel zone strength that assures sufficient plastic rotation capacity while reducing the amount of beam buckling is proposed. Numerical studies to supplement the test results are then presented based on the validated finite element analysis. Satisfactory numerical simulation achieved in this study also indicates that numerical analysis based on quality finite element modeling can supplement or replace, at least in part, the costly full-scale cyclic testing of steel moment connections.

**Key words** steel moment connections, panel zone, reduced beam section, seismic design

## 1. Introduction

In response to the widespread damage in connections of steel moment-resisting frames that occurred during the 1994 Northridge and the 1995 Kobe earthquakes, a number of improved beam-to-column connection design strategies have been proposed. Of a variety of new designs, the

reduced beam section (RBS) connection has been shown to exhibit satisfactory levels of ductility in numerous tests and has found broad acceptance in a relatively short time. However, there still remain several design issues that should be further examined.<sup>(1,2)</sup> One such issue is the optimal panel zone strength. Although a significant amount of test data are available, a specific recommendation for a desirable range of panel zone strength versus beam strength has not been proposed. In the first part of this paper, after summarizing the effects of panel zone strength on the cyclic performance of RBS connection, a criterion for a balanced panel zone strength is proposed

<sup>1)</sup> 정회원·서울대학교 건축학과 부교수 (대표지자: ceholee@snu.ac.kr)

<sup>2)</sup> 서울대학교 건축학과, 박사과정

본 논문에 대한 토의를 2006년 8월 31일까지 학회로 보내 주시면 그 결과를 게재하겠습니다.

(논문접수일 : 2006. 5. 19 / 심사종료일 : 2006. 5. 25)

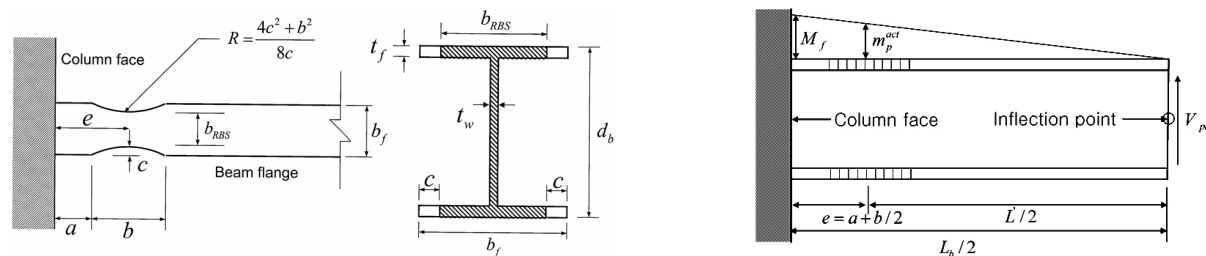
based on the author's recent study.<sup>(3)</sup> Next, numerical studies conducted to supplement the test results are also presented.

## 2. Summary of Experimental Observations

### 2.1 Testing Program by Lee et al.<sup>(3)</sup>

The experimental observations from the testing program by Lee et al.<sup>(3)</sup> are briefly summarized in the following. A total of six full-scale test specimens were designed with the panel zone strength as the key test variable (see

Table 1). Typical geometry and seismic moment profile for the design of the radius-cut RBS are shown in Fig. 1. The grade of steel for the beams was SS400 with a specified minimum yield strength of 235 Mpa (34 ksi); SM490 steel was used for the columns and the specified minimum yield strength was 324 Mpa (47 ksi). The RBS design followed the recommendations by Iwankiw and Engelhardt et al.<sup>(4,5)</sup> The strain hardened plastic moment at the RBS hinge was calculated using the expected yield strength ( $F_{ye} = R_y \times F_y = 1.33 \times 235 = 313 \text{ Mpa}$ ) and a strain hardening factor of 1.1.



〈Figure 1〉 Typical geometry and seismic moment profile for RBS design.

〈Table 1〉 Test Specimens

Specimen	Beam and column (Equivalent US W- section )	PZ strength ratio <sup>a)</sup>	Beam web connection method	a (mm)	b (mm)	c (mm)	Flange reduction (%)
DB700-MW	H700X300X13X24 (W27X123) H428X407X20X35 (W17X271)	Medium (0.87)	Welded	175	525	55	37
DB700-SW	H700X300X13X24 (W27X123) H428X407X20X35 (W17X271)	Strong (Not Available)	Welded	175	525	55	37
DB600-MW1	H600X200X11X17 (W24X70) H400X400X13X21 (W16X115)	Medium (0.83)	Welded	150	510	40	40
DB600-MW2	H600X200X11X17 (W24X70) H400X400X13X21 (W16X115)	Medium (0.82)	Welded	150	390	40	40
DB600-SW1	H600X200X11X17 (W24X70) H588X300X12X20 (W24X100)	Strong (0.66)	Welded	150	450	40	40
DB600-SW2	H606X201X12X20 (W24X80) H588X300X12X20 (W24X100)	Strong (0.63)	Welded	150	450	40	40

<sup>a)</sup> Based on the strength ratio  $V_{RBS,p}/V_p$ ,  $V_{RBS,p}/V_p$ ; refer to Eqs. 4 and 8 for definition

$$m_p^{act} = \alpha \times Z_{RBS} \times F_{yc} = (1.1) \times Z_{RBS} \times F_{yc} \quad (1)$$

The corresponding seismic moment at the face of the column is

$$M_f = m_p^{act} \left( \frac{L_b}{L'} \right) \quad (2)$$

In this study, the trimmed flanges were sized to limit the moment at the column face to about 90 percent of  $M_p$ . The panel zones were then designed for  $m_p^{act}$  at the RBS hinge by using either of the following two equations for the panel zone design shear strength:

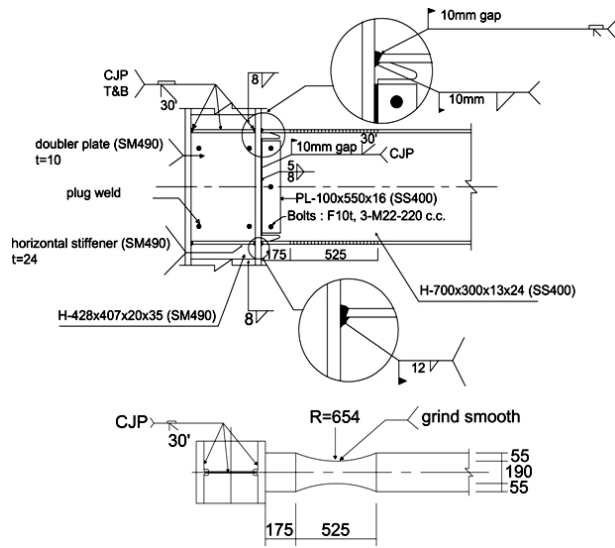
$$V_p = (0.75)(0.6F_{yc}d_c t_p) \left[ 1 + \frac{3b_{cf}t_{cf}^2}{d_b d_c t_p} \right] \quad (3)$$

$$V_p = (0.6F_{yc}d_c t_p) \left[ 1 + \frac{3b_{cf}t_{cf}^2}{d_b d_c t_p} \right] \quad (4)$$

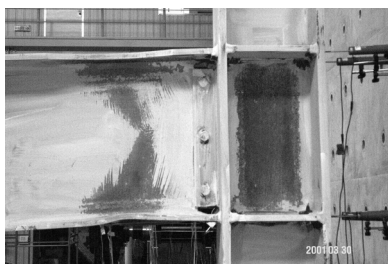
where  $F_{yc}$  = yield strength of the column,  $d_b$  = beam

depth,  $d_c$  = column depth,  $t_p$  = thickness of the panel zone,  $b_{cf}$  = column flange width, and  $t_{cf}$  = column flange thickness. Eq. (4), which is adopted in the 2002 AISC Seismic Provisions, was used to design the medium panel zone specimens. This equation represents the panel zone shear strength when the shear strain reaches 4 times the shear yield strain.<sup>(6)</sup> Eq. (3), which includes a strength reduction factor of 0.75, was implemented in the 1997 AISC Seismic Provisions. Specimens with panel zone designed by Eq. (3) are defined as the strong panel zone specimens in this study because inelastic rotation is expected to develop mainly in the beam. When Eq. (3) was used for the panel zone strength, a doubler plate of 10 mm thickness was provided for specimen DB700-SW. The doubler plates were plug-welded to the column web to prevent premature local buckling.<sup>(7)</sup> All the beam webs were groove-welded to the column flange. Continuity plates equal in thickness to the beam flange were provided in all specimens. Electrodes with a specified minimum Charpy V-Notch (CVN) toughness of 26.7 Joule at  $-28.9^\circ\text{C}$  ( $20^\circ\text{F}$ ) was specified for flux-cored arc welding. Weld access hole configurations followed the SAC recommendations.<sup>(8)</sup> In Table 1, the following abbreviations were used for the specimen designation: S = strong panel zone, M = medium panel zone, and W = welded web. Fig. 2 shows the connection details for specimen DB700-SW.

The specimens were mounted to a strong floor and a strong wall. Lateral restraint was provided at a distance of 2500 mm from the column face. The specimens were tested statically according to the SAC standard loading protocol.<sup>(9)</sup> Both strong and medium panel zone specimens developed satisfactory levels of ductility (4% drift) required of special moment frames. Significant yielding of



⟨Figure 2⟩ Specimen DB700-SW moment connection details.

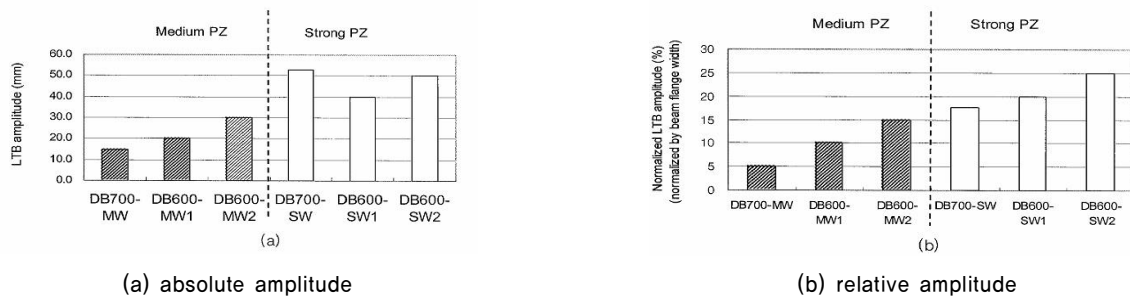


(a) DB700-MW at 5% story drift



(b) DB700-SW at 6% story drift

⟨Figure 3⟩ Comparison of connection regions.



〈Figure 4〉 Comparison of LTB amplitudes at 4% story drift cycle.

the panel zone in specimen DB700-MW was evident from the flaking of the whitewash (Fig. 3a). Specimen DB700-SW exhibited excellent rotation capacity, but with experiencing significant beam buckling (Fig. 3b).

Fig. 4 presents a comparison of the measured beam lateral-torsional buckling (LTB) amplitudes up to the 4% story drift cycles. The LTB amplitudes were measured based on the buckled flange shape. Because panel zone contributed less to plastic rotation in the strong panel zone specimens, LTB amplitudes of these beams were larger. Since a well designed RBS connection would fracture eventually by low-cycle fatigue fracture of the beam flanges in the RBS region for drift beyond 4% and such fracture is associated with very large curvatures due to buckling, a reduction of the LTB amplitude implies both less post-earthquake damage and a less tendency for beam flange fracture.

## 2.2 Further Analysis Including Other Independent Testing Programs

For the purpose of analyzing the effects of panel zone strength, Krawinkler's recommendation (Eq. 4), which includes the column flange contribution (CFC) to the post-yield strength, was used as a measure of the panel zone strength. Heavy columns with thicker and wider flanges will benefit more from the higher resistance provided by this second term. As a measure of the beam strength, the panel zone shear force  $V_{RBS,p}$  corresponding to the development of the actual plastic moment of the RBS was used such a measure was also used by Roeder.<sup>(10)</sup> For a one-sided moment connection,  $V_{RBS,p}$  can be computed as follows:

$$V_{RBS,p} = \left( \frac{M_{RBS,p}}{d_b} \right) \times \left( \frac{L_b/2 + d_c/2}{L_b/2 - e} \right) \times \left( 1 - \frac{d_b}{H_c} \right) \quad (5)$$

where  $M_{RBS,p}$  = plastic moment at the RBS based on the measured yield strength,  $H_c$  = column height. Refer to Fig. 2 for the remaining symbols. For a two-sided moment connection configuration with the same beam size and span length on both sides of the column,  $V_{RBS,p}$  is twice the value given by Eq. (5). Once the beam strength is expressed in the form of  $V_{RBS,p}$ , the relative strength between the beam and the panel zone can be measured by the ratio  $V_{RBS,p}/V_p$  a lower value implies a stronger panel zone.

To augment the database, test results from Engelhardt et al.<sup>(5,11)</sup>, Tsai and Chen<sup>(12)</sup>, Yu et al.<sup>(13)</sup>, Chi and Uang<sup>(1)</sup>, and Jones et al.<sup>(2)</sup> were included. The test data comprised both bare steel and composite specimens with various column and beam sizes; all specimens were able to develop satisfactory connection rotation capacity for special moment-resisting frames. The panel zone strength ranges from very weak to very strong. Several observations from the augmented test data are summarized in the following.

### 2.2.1 Energy Dissipation and Plastic Rotation by the Panel Zone

Specimens with a weaker panel zone consistently dissipated more energy through the panel zone yielding. Up to 4% story drift cycle, Specimens specimens with  $V_{RBS,p}/V_p = 0.70 \sim 0.90$  developed about 0.01 rad. plastic rotation and dissipated about 30%~40% of the total energy up to 4% story drift cycle. Due to the bracing effect provided by the composite floor slab, composite specimens exhibited a greater strength (about 10% on

average) and energy dissipation (often more than twice) than their bare steel counterparts.

### 2.2.2 Behavior of Specimens with Very Strong or Very Weak Panel Zones

Two strong panel zone specimens (4B and 4C,  $V_{RBS,p}/V_p = 0.56$ ) tested by Jones et al.<sup>(2)</sup> dissipated a considerably less amount of energy than the other specimens. One consequence of the strong panel zone design was that all energy dissipation was concentrated in the RBS region, while caused a significant amount of buckling. Lateral-torsional buckling of the beams then caused column twisting, thus preventing the specimens from developing sufficient ductility.<sup>(1,2,11)</sup>

The problem of strong panel zone design mentioned above can be somewhat alleviated if the panel zone is also designed to yield. In the extreme case, a very weak panel zone design would result in a situation where the beam would remain elastic while all the inelasticity action occurs in the panel zone. This was the case for specimens 3B and 3C tested by Jones et al.<sup>(2)</sup> Both specimens showed very stable hysteretic response before the beams fractured at large drift levels. The plastic rotation developed in the panel zone ranged from 0.034 to 0.038 radian. Large rotations in the panel zone were accompanied by kinking of the column flanges at the four corners of the panel zone. Tests on free flange moment connection conducted by Choi et al.<sup>(14)</sup> also revealed similar problems associated with the very weak or very strong panel zone design; excessive panel zone yielding of the weak panel zone specimens eventually fractured the beam flange while severe out-of-plane deformation was observed after the beam web yielding in the strong panel zone specimens.

Although weak panel zone design has been studied and available test data showed stable cyclic response<sup>(15,16)</sup>, this design approach is not favored for the welded moment connection design for the following concerns. First, kinking of the column flanges not only produces complex triaxial stress conditions but also increases the potential for fracture in the beam flange welds.<sup>(17)</sup> Second, weak panel zone design would result in a lower system overstrength of the structure; system overstrength plays

an important role for the survival of a structure during a major earthquake.<sup>(18)</sup>

Based on the observations presented above, a balanced panel zone strength ratio was proposed by Lee et al.<sup>(3)</sup> such that problems associated with the use of either a strong or a weak panel zone can be avoided. Test results showed that a properly designed panel zone can easily develop a plastic rotation of about 0.01 radian, without distressing the beam flange groove welds, with reduced beam buckling when  $V_{RBS,p}/V_p$  is in the following range:

$$0.70 \leq \frac{V_{RBS,p}}{V_p} \leq 0.90 \quad (6)$$

The balanced panel zone design proposed will also lead to the reduction of expensive doubler plates (and thus the reduction of cracking-prone k area welding), especially for two-sided moment connections with massive beams.

## 3. Supplemental Numerical Studies

### 3.1 Finite Element Modeling and Verification

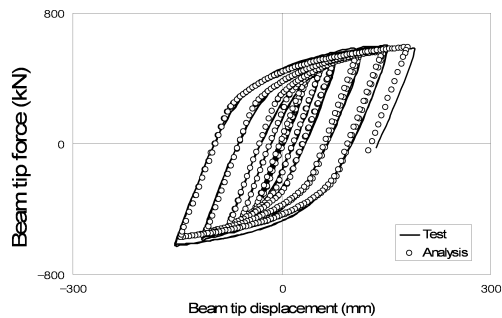
To gain further insight into the effects of the panel zone strength on the cyclic behavior of the RBS connection, nonlinear finite element analysis was conducted. Four specimens (DB700-MW, DB700-SW, DB600-MW1, DB600-SW1) tested by Lee et al.<sup>(3)</sup> were modeled and analyzed by using the general purpose finite element analysis program ABAQUS.<sup>(19)</sup> Achieving high-profile cyclic correlation of the finite element analysis results with the test results of the four specimens was among the most significant consideration in this numerical study. Both the flanges and the web of the beam and the column were modeled with the quadrilateral four-node shell element (element S4R in ABAQUS). Material nonlinearity with the von Mises yielding criterion combined with nonlinear isotropic/kinematic hardening model was considered in the cyclic analysis. Steel material properties followed the results of tensile coupon tests. The initial kinematic hardening modulus and rate of kinematic hardening decrease were calibrated based on the test data by Kaufmann et al.<sup>(20)</sup> To simulate local buckling and



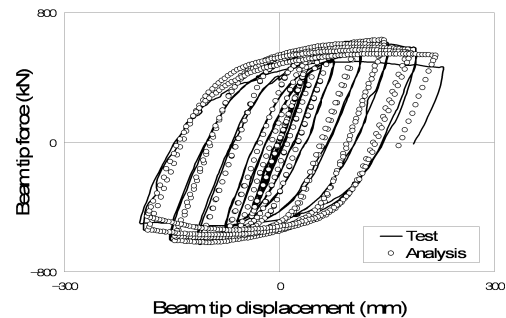
lateral torsional buckling, geometric imperfections based on the first buckling mode were introduced by perturbations in the geometry. Cyclic displacement history was imposed to the beam end according to the SAC 2000 standard loading protocol. The modified RIKS algorithm was used so that unstable postbuckling response could be

traced.

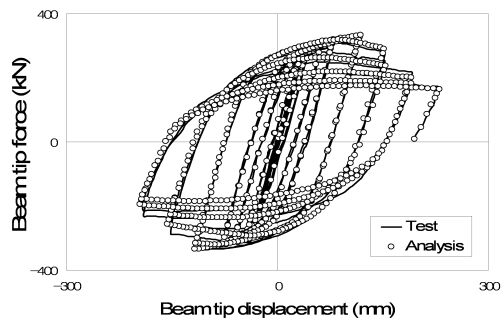
To examine the overall validity of the finite element model to be used, various response parameters were compared. Fig. 5 shows that the analytically predicted cyclic load versus beam tip displacement relationship correlated well with the experimental relationship. Baus-



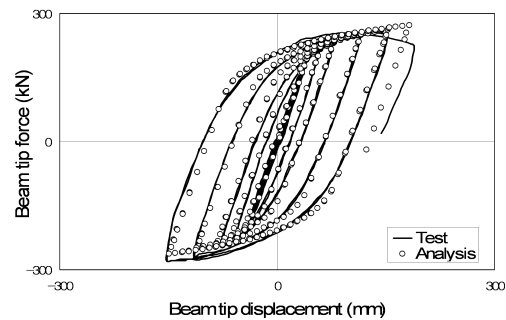
(a) DB700-MW



(b) DB700-SW

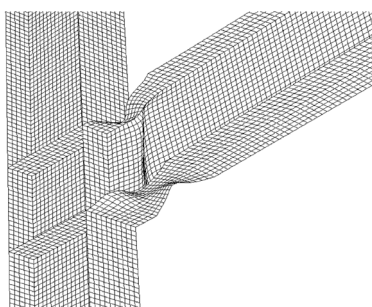


(c) DB600-SW1

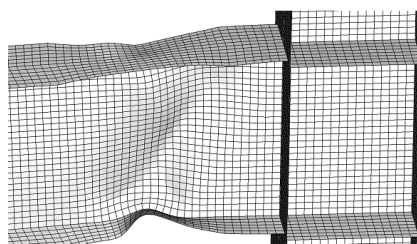


(d) DB600-MW1

〈Figure 5〉 Correlation of analytical and experimental cyclic load-displacement relationships.



(a) DB600-SW1



(b) DB700-SW



〈Figure 6〉 Comparison of predicted and experimental deformed configuration.

chinger effect, cyclic strain-hardening, and the strength degradation due to local and lateral torsional buckling were well simulated. The predicted deformation configuration near the connection was also reasonably comparable to that of the test (Fig. 6).

Comparisons of other response parameters are summarized in Table 2. The analytically predicted plastic rotations correlated well with the experimental results. Local and lateral torsional buckling amplitudes were also well simulated by the analysis in the strong panel zone models (DB700-SW and DB600-SW1). However the prediction accuracy tended to degrade in the case of the buckling amplitude of the medium panel zone models (DB700-MW and DB600-MW1). This inconsistency might

be due to the difference in the degree of lateral restraint between the analysis model and the test condition; a gap of 5~10 mm between the beam flange and the lateral support was needed to set up the specimen in the test, but no gap was assumed in the analysis. Total energy dissipation in the connection was also well compared. Relative energy dissipation between the beam and the panel zone was reasonably predicted. Overall, the finite element analysis model of this study can simulate the cyclic behavior of the RBS connection with reasonable accuracy.

### 3.2 Numerical Analysis of PZ Strength Effects

Based on the satisfactory correlation study presented above, parametric finite element analyses were conducted.

(Table 2) Comparison of experimental and numerical responses (at the end of 4% story drift cycle).

		DB700-MW		DB700-SW		DB600-MW1		DB600-SW1	
		Test	Analysis	Test	Analysis	Test	Analysis	Test	Analysis
Total energy dissipation (kJ)		803.6	792.2	901.4	857.6	400.1	380.4	446.2	434.4
Component energy dissipation (kJ)	Beam	459.8 (57.2%)	462.7 (58.4%)	720.3 (79.9%)	689.3 (80.3%)	266.1 (66.5%)	242.3 (63.7%)	354.5 (79.4%)	332.6 (76.6%)
	Panel zone	327.3 (40.7%)	320.8 (40.5%)	180.1 (20%)	166.2 (19.4%)	122.8 (30.7%)	133.9 (35.2%)	88.6 (19.9%)	98.5 (22.7%)
	Column	16.5 (2.1%)	8.7 (1.1%)	1.0 (0.1%)	2.1 (0.3%)	11.2 (2.8%)	4.2 (1.1%)	3.1 (0.7%)	3.3 (0.7%)
Component plastic rotation (rad)	Beam	0.017	0.016	0.026	0.023	0.018	0.017	0.032	0.027
	Panel zone	0.012	0.011	0.0003	0.005	0.013	0.010	0.0001	0.0001
	Column	0.0002	0.0004	0.0001	0.0003	0.0002	0.0005	0.0003	0.00002
Buckling amplitude (cm)	LTB	1.5	0.6	5.0	4.3	0.5	0.09	4.0	4.5
	FLB	Not available	0.01	Not available	0.7	3.0	0.8	5.0	4.3
	WLB	2.0	0.8	5.3	4.8	3.0	1.2	7.0	6.0

(Table 3) Comparison of numerical analysis results of DB700 series (at the end of 4% story drift cycle).

Response parameters		DB700-S ( $V_{RBS,P}/V_P=0.63$ ) Strong PZ	DB700-M ( $V_{RBS,P}/V_P=0.87$ ) Balanced PZ	DB700-W ( $V_{RBS,P}/V_P=1.14$ ) Weak PZ
Total energy dissipation (kJ)		857.6	792.2	722.8
Component energy dissipation (kJ)	Beam	689.3 (80.3%)	462.7 (58.4%)	1.3 (0.3%)
	Panel zone	166.2 (19.4%)	320.8 (40.5%)	632.3 (87.4%)
	Column	2.1 (0.3%)	8.7 (1.1%)	89.2 (12.3%)
Component plastic rotation (rad)	Beam	0.023	0.016	0.0003
	Panel zone	0.005	0.011	0.028
	Column	0.0003	0.0004	0.004
Buckling amplitude (cm)	LTB (cm)	4.3	0.6	Almost zero
	FLB (cm)	0.7	0.01	Almost zero
	WLB (cm)	4.8	0.8	Almost zero

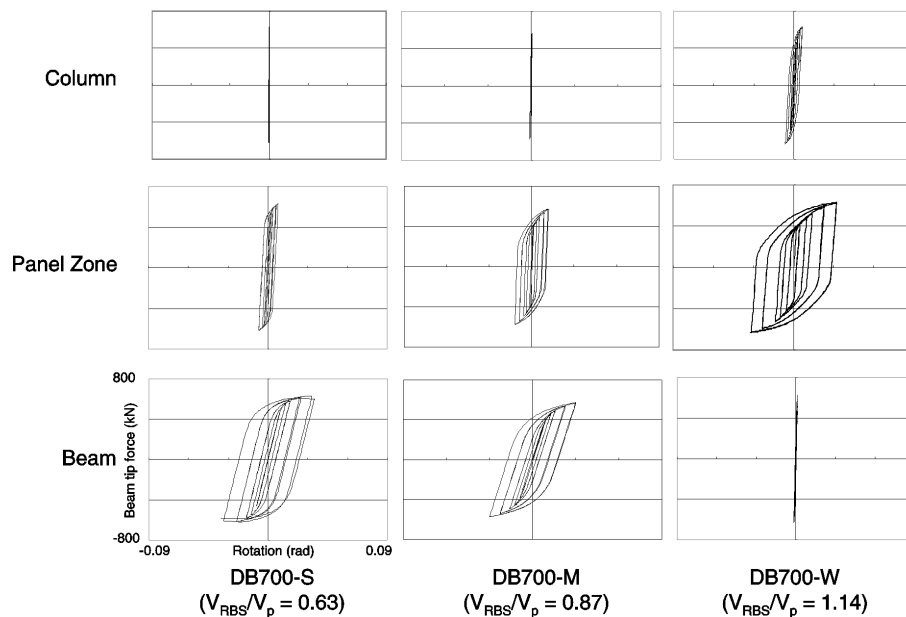
By changing the panel zone strength of specimens DB700-MW and DB600-SW2, a total of 6 finite element models with strong, balanced, and weak panel zone were prepared and analyzed. The numerical analysis results of DB700 and DB600 series are summarized in Table 3 and Table 4, respectively. Figures 7 and 8 show the comparison of the beam tip force versus component rotation relationships.

These analytical results reproduced the same tendency as that experimentally observed. In the strong panel zone models, the beam dissipated most of the energy with

experiencing significant beam buckling (and also strength degradation). In the balanced panel zone model, the panel zone dissipated 30~40% of the total energy. Note that the energy dissipation by the column is negligible in the balanced panel zone model ( $V_{RBS,p}/V_p = 0.87$ ). However, in the weak panel zone model ( $V_{RBS,p}/V_p = 1.14$ ), the panel zone dissipated most of the energy with accompanying the column hinging (or local yielding of the column flanges at the continuity plates level). Fig. 9 shows the column hinging formed in the weak panel zone model (DB700-W). The numerical simulation results

〈Table 4〉 Comparison of numerical analysis results of DB600 series (at the end of 4% story drift cycle).

Response parameters		DB600-S ( $V_{RBS,p}/V_p = 0.62$ ) Strong PZ	DB600-M ( $V_{RBS,p}/V_p = 0.82$ ) Balanced PZ	DB600-W ( $V_{RBS,p}/V_p = 1.13$ ) Weak PZ
Total energy dissipation (kJ)		443.4	380.4	357.8
Component energy dissipation (kJ)	Beam	332.6 (76.6%)	242.3 (63.7%)	2.7 (0.7%)
	Panel zone	98.5 (22.7%)	133.9 (35.2%)	305.9 (85.5%)
	Column	3.3 (0.7%)	4.2 (1.1%)	49.2 (13.7%)
Component plastic rotation (rad)	Beam	0.027	0.017	0.0003
	Panel zone	0.0001	0.010	0.028
	Column	0.00005	0.0005	0.004
Buckling amplitude (cm)	LTB (cm)	4.5	0.09	Almost zero
	FLB (cm)	4.3	0.8	Almost zero
	WLB (cm)	6.0	1.2	Almost zero



〈Figure 7〉 Comparison of beam tip force versus component rotation relationships (DB700 series).



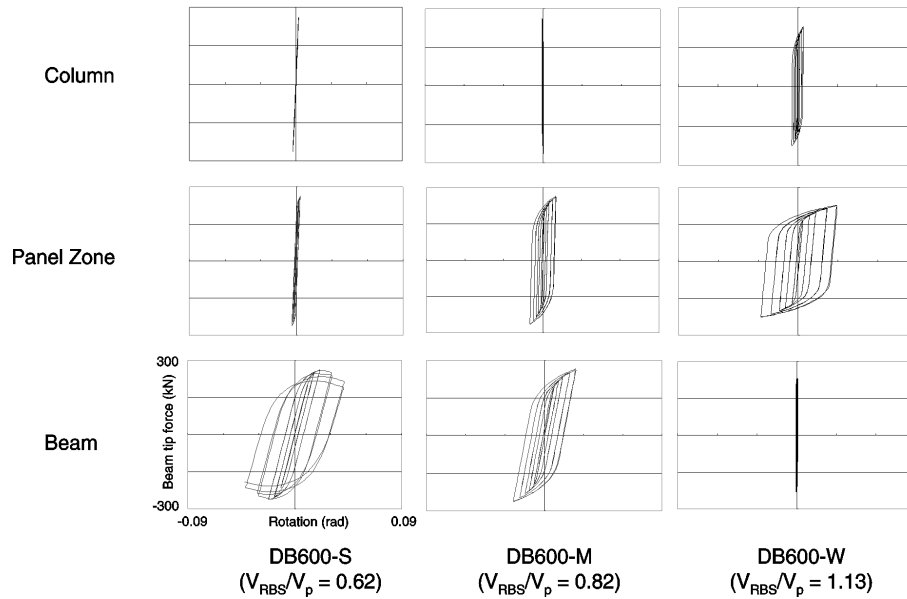


(Figure 8) Comparison of beam tip force versus component rotation relationships (DB600 series).

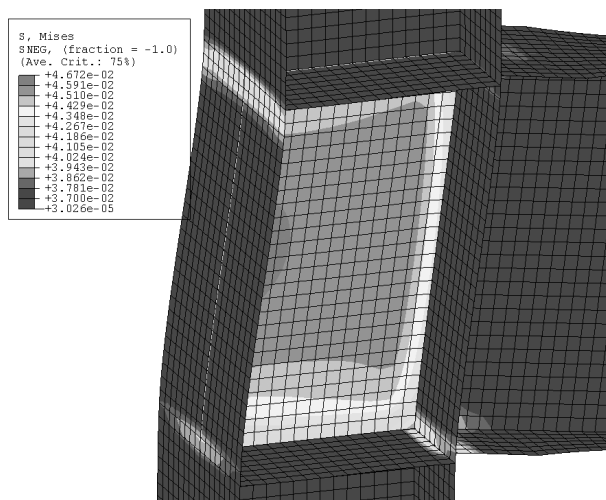


(Figure 9) Column flange yielding in the weak panel zone model (DB700-W).

of this study also imply that calibrated and quality finite element analysis can supplement or replace, at least in part, the costly full-scale cyclic testing of steel moment connections.

#### 4. Conclusions

Effects of the panel zone strength on cyclic performance of the RBS connection were investigated based on the experimental and numerical results. The following conclusions can be made.

- (1) Both strong and medium panel zone specimens with a well design RBS connection exhibited satisfactory levels of connection ductility required of special moment-resisting frames. But specimens that were designed for a strong panel zone experienced more significant beam buckling and larger permanent distortions because inelastic action was concentrated in the RBS region. But using a very weak panel zone is also not favored due to concerns of potential weld fracture associated with the kinking of column flanges. A criterion for a balanced PZ strength is proposed such that problems associated with the use of either a strong or a weak panel zone can be avoided.
- (2) The finite element models of this study were able to simulate various cyclic response parameters of the RBS connection satisfactorily. The validated finite element analysis results showed that energy dissipation by the column hinging is negligible when following the balanced panel zone strength criterion proposed. However, even in the slightly weak panel zone model (relative strength ratio of  $V_{RBS,p} / V_p = 1.14$ ), the column hinging was unavoidable; the column had to dissipate more than 10% of the total energy.

#### Acknowledgment

Financial support provided by the Korea Earthquake

Engineering Research Center (KEERC) (Project No: R11-1997-045-11004-0) is gratefully acknowledged.

## References

1. Chi, B. and Uang, C.-M., "Cyclic response and design recommendations of reduced beam section moment connections with deep column," *J. Struct. Engrg.*, ASCE, 128(4), 2002, pp. 464-473.
2. Jones, S. L., Fry, G. T., and Engelhardt, M. D., "Experimental evaluation of cyclically loaded reduced beam section moment connections," *J. Struct. Engrg.*, ASCE, 128(4), 2002, pp. 441-451.
3. Lee, C.-H., Jeon, S.-W., Kim, J.-H., and Uang, C.-M., "Effects of panel zone strength and beam web connection method on seismic performance of reduced beam section steel moment connections," *J. Struct. Engrg.*, ASCE, 131(12), 2005, pp. 1854-1865.
4. Iwankiw, N., "Ultimate strength consideration for seismic design of the reduced beam section (internal plastic hinge)," *Engrg. J.* 34(1), AISC, First Quarter, 1997, pp. 3-16.
5. Engelhardt, M. D., Winneberger, T., Zekany, A. J., and Potyraj, T. J., "Experimental investigations of dogbone moment connections," *Engrg. J.*, 35(4), AISC, Fourth Quarter, 1998, pp. 128-139.
6. Krawinkler, H., "Shear in beam-column joints in seismic design of steel frames," *Engrg. J.*, 15(3), AISC, Third Quarter, 1978, pp. 82-91.
7. American Institute of Steel Construction (AISC), *Seismic provisions for structural steel buildings*, American Institute of Steel Construction, Chicago, IL., 1997 and 2002.
8. SAC, *Seismic design criteria for new moment-resisting steel frame construction, Report No. FEMA 350*, SAC Joint Venture, Sacramento, Calif., 2000.
9. Krawinkler, H., Gupta, A., Medina, R., and Ruco, N., *Loading histories for seismic performance testing of SMRF components and assemblies, Report No. SAC/BD-00/10*, SAC Joint Venture, Sacramento, Calif., 2000.
10. Roeder, C. W., "General issues influencing connection performance," *J. Struct. Engrg.*, ASCE, 128(4), 2002, pp. 420-428.
11. Engelhardt, M. D., Venti, M. J., Fry, G. T., Jones, S. L., and Holliday, S. D., *Behavior and design of radius cut reduced beam section connections, SAC/BD-00/17*, SAC Joint Venture, Sacramento, Calif., 2000.
12. Tsai, K. C. and Chen, W.-Z., "Seismic response of steel reduced beam section to weak panel zone moment joints," *Proc. Third International Conference STESSA 2000*, 21-24 August, Montreal, Canada, 2000.
13. Yu, Q. S., Gilton, C., and Uang, C.-M., *Cyclic response of RBS moment connections: loading sequence and lateral bracing effects, SAC/BD-00/22*, SAC Joint Venture, Sacramento, Calif., 2000.
14. Choi, J. H., Stojadinovic, B., and Goel, S. C., *Development of free flange moment connection, Technical Report UMCEE 00-15*, Dept. of Civil and Environmental Engineering, Univ. of Michigan, Ann Arbor, Mich., 2000.
15. Kawano, A., "Inelastic behavior of low-rise frame based on a weak beam-to-column connection philosophy to earthquake motion," *Proc. Eighth World Conference on Earthquake Engineering*, Vol. IV, San Francisco, Calif., 1984.
16. Suita, K., Inoue, K., and Kanoh, N., "Strength and deformation of bolted beam-to-column connection accompanied by panel zone yield," *Proc. Fourth Taiwan-Japan-Korea Joint Seminar on Earthquake Engineering for Building Structures*, Oct. 25-26, Seoul, Korea, 2002.
17. El-Tawil, S., "Panel zone yielding in steel moment connections," *Engrg. J.*, 37(3), AISC, Third Quarter, 2000, pp. 120-131.
18. Uang, C.-M., "An evaluation of two-level seismic design procedure," *Earthquake Spectra*, 9(1), 1993, pp. 121-135.
19. ABAQUS User's Manual, Vols. I and II, Version 6.2 Hibbit, Karlson & Sorenson, Inc., 2001.
20. Kaufmann, E. J., Metrovich, B., and Pense A. W., "Characterization of cyclic inelastic strain behavior on properties of A572 Gr. 50 and A913 Gr. 50 rolled sections," *Final Report to American Institute of Steel Construction, ATLSS*, Leigh University, PA., 2001.